

Reduced levels of heparan sulfate in cerebrospinal fluid reflect correction of brain neurons in mucopolysaccharidosis type III mice

Steven Q. Le, Alexander Sorensen, Soila Sukupolvi, Gianna Jewthorst, Grant Austin, Balraj Doray, Jonathan D. Cooper, Patricia I. Dickson

Department of Pediatrics, Washington University School of Medicine, St. Louis, MO

Supplemental Material

Methods

Sex as a biological variable. We studied male and female mice as reported in the Figure Legend. We did not observe sex-specific differences in the outcomes we assessed.

Reagents. Human mucopolysaccharidosis (MPS) type IIIB fibroblasts (GM 1426) were obtained from Coriell. The *Naglu*^{-/-} mouse model was originally obtained from Elizabeth Neufeld (1). 4-methylumbelliferyl-*N*-acetyl- α -glucosaminide and 4-methylumbelliferyl-*N*-acetyl- β -glucosaminide were obtained from EMD Millipore Chemicals (Darmstadt, Germany). TrueBlack Lipofuscin Autofluorescence Quencher was obtained from Biotium. Primary antibodies used in this study were rabbit anti- α -*N*-acetylglucosaminidase (NAGLU; ab214671, abcam), mouse anti-NeuN (MAB377, Sigma), anti-mouse glial fibrillary acidic protein (GFAP; G3893, Sigma), and anti-rat CD68 (MCA1957, Biorad). Secondary antibodies purchased from Thermofisher were goat-anti rabbit 488 (A11008), goat anti-mouse 546 (A-11003), and goat anti-rat 647(A-21247).

Viral vectors. The adeno-associated viral (AAV) vectors used in this study were constructed either by inserting the transgene NAGLU-LAMP1 (where LAMP1 is lysosome-associated membrane protein 1) into an AAV-CBA backbone containing the cytomegalovirus (CMV) enhancer/chicken beta actin (CBA) promoter, or an AAV vector driven by the neuron-specific synapsin 1 promoter (Syn1). The synapsin-1 promoter has been shown to also express in liver (2, 3), which may explain the presence of low amounts of NAGLU activity and reduction in beta-hexosaminidase activity in liver in mice that received the higher vector dose. The NAGLU-LAMP1 transgene construct consists of the human NAGLU cDNA joined via a linker nucleotide sequence (encoding six glycine residues) to a 114-bp nucleotide segment corresponding to the transmembrane region and cytosolic tail of LAMP1. Nucleotides encoding the c-Myc epitope tag

were appended to the cytosolic tail of LAMP1. The NAGLU-LAMP1 transgene was initially cloned into a commercially available lentiviral (LV) vector, Lenti-III-pGK (G305, abm) to generate LV-NAGLU-LAMP1 to test transduction in vitro. For mouse studies, the NAGLU-LAMP1 transgene in the AAV vectors were packaged into either the AAV7 serotype (for CBA NAGLU-LAMP1) or the AAV9 serotype (for Syn1 NAGLU-LAMP1) and produced by the Hope Center Viral Vectors Core at Washington University School of Medicine. The AAV7-CBA-NAGLU-LAMP1-myc viral titer was 1.5E13 viral genomes per ml, while the AA9-Syn1-NAGLU-LAMP1-myc viral titer was 1.3E13 viral genomes per ml.

Cell culture. Human MPS IIIB fibroblasts were transduced with LV-NAGLU-LAMP1 and selected with 10 µg/ml puromycin added to the culture media. Cells and media were harvested and tested for NAGLU and beta-hexosaminidase activity as described below.

Mice. All experiments in this study were performed using the *Naglu*^{-/-} mouse strain B6.129S6-Naglu(tm1Efn)/J (1). Mice were bred by crossing knockout males to heterozygous females, producing 50% knockout and 50% heterozygous offspring. Genotyping was performed at birth with primer set NAG5': TGGACCTGTTTGCTGAAAGC and NAG3':

CAGGCCATCAAATCTGGTAC for *Naglu* wild-type alleles, and primer set Neo5':

TGGGATCGGCCATTGAACAA; Neo3': CCTTGAGCCTGGCGAACAGT for *Neo*' mutant

alleles. Intravenous dosing of AAV7-NAGLU-LAMP1 was performed by tail vein injection.

Intracerebroventricular dosing of AAV9-Syn1-NAGLU-LAMP1 was performed by

intracerebroventricular injection in neonatal mice as described (4). For intraventricular dosing of

AAV9-Syn1-NAGLU-LAMP1, mice were cryoanesthetized, and viral vector was injected at 5 µl

volume using a 32-gauge Hamilton syringe. Terminal cerebrospinal fluid collection was

performed by cisterna magna puncture. Blood was obtained by cardiac puncture, following

which mice were perfused transcardially with chilled PBS. Brain left hemisphere, liver, kidneys, and heart were collected and snap frozen for biochemical assays. The brain right hemisphere was fixed in paraformaldehyde for histology.

Enzymatic activity assays. Samples were coded so that assays could be performed in a blinded fashion. NAGLU activity and total hexosaminidase activity were quantified using 4-methylumbelliferyl assays as previously described (4). Briefly the enzymatic activity of NAGLU was determined by hydrolysis of the fluorogenic substrate, 4-methylumbelliferyl-*N*-acetyl- α -glucosaminide, obtained from EMD Millipore Chemicals (Darmstadt, Germany) with minor modifications of a published protocol, using 0.1 mM substrate in the incubation mixture (5). Enzymatic activity of beta-hexosaminidase (combined A and B isoforms) was determined by hydrolysis of 4-methylumbelliferyl-*N*-acetyl- β -glucosaminide (EMD Millipore Chemicals, Darmstadt, Germany) using 1.25 mM substrate in the incubation mixture. For both enzymes, a unit of activity is defined as release of 1 nmol of 4-methylumbelliferone (4MU) per hour. Protein concentration was estimated by the Bradford method, using bovine serum albumin as a standard.

Heparan sulfate (HS) quantification. Samples were sent to the University of California San Diego GlycoAnalytics core for evaluation of HS levels by mass spectrometry. Samples were coded so that assays were performed in a blinded fashion. For HS analysis, tissue homogenates, cerebrospinal fluid, and serum samples were treated with protease and the negatively charged glycosaminoglycans were trapped using Anion Exchange Chromatography (AEC). Bound glycosaminoglycans were eluted with high concentration of chloride as counter ion (2M NaCl solution) followed by desalting using pre-packed desalting column (PD-10). Purified total glycosaminoglycans were digested with mixture of Heparinase (I, II & III) which depolymerize the chains, generating mostly disaccharides. The disaccharides were tagged with $^{12}\text{C}_6$ -aniline by

reductive coupling method (termed as Glycan Reductive Isotopic Labeling, GRIL)(6). These aniline-tagged disaccharide mixtures were spiked with known amounts of $^{13}\text{C}_6$ -isotopic aniline tagged disaccharide standard mixture and analyzed using Liquid Chromatography Mass Spectrometry (LC-MS) in negative ionization mode (LTQ-Orbitrap Discovery, Thermo Scientific). The ion intensities of the standards and the samples that coelute were deconvoluted by mass spectrometry and quantified.

Immunostaining. Brains were post-fixed overnight in PFA and cryoprotected in 30% sucrose/50 mM tris-buffered saline (TBS) at 4 °C. Samples were coded so that histology was performed in a blinded fashion. A 1-in-6 series of 40 μm coronal forebrain hemisections from each mouse were collect in 96-well plates containing a cryoprotectant solution (TBS/30% ethylene glycol/15% sucrose/0.05% sodium azide). Sections were subsequently mounted and stained on slides using the TrueBlack Lipofuscin Autofluorescence Quencher (Biotium) and immunofluorescently stained using 1° antibody and 2° antiserum in TBST with 10% normal serum as described previously (7-9). Primary antibodies are listed in the Reagents section above and included rabbit anti-NAGLU, mouse anti-NeuN, mouse anti-GFAP, and rat-CD68, with corresponding secondary antibodies goat anti rabbit 488, goat anti-mouse 546 and goat anti-rat 647. Stained slides were scanned using a Zeiss Axio Imager.Z1 microscope and processed with the StereoInvestigator (MBF Bioscience) software, and quantification of immunoreactivity for each antigen was performed via thresholding using ImagePro Premier as described (7-9).

Statistical analysis. We used STATA 17 (College Station, Texas) to perform analysis of variance for categorical variables using the “anova” command. We performed post-hoc pairwise comparisons using the “pwmean” command. A *P* value less than 0.05 was considered significant.

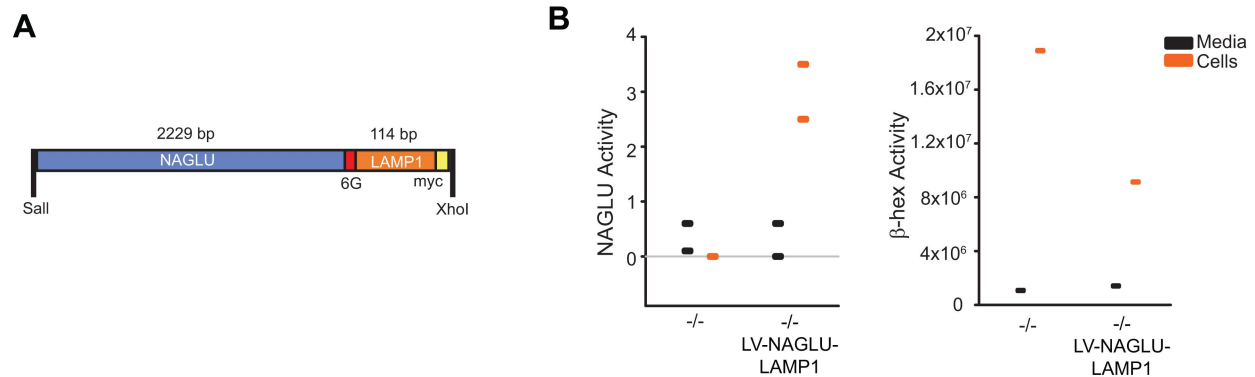
Study approval. All study procedures involving mice were in full compliance with the National Institutes of Health's Guide for the Care and Use of Laboratory Animals and approved by the Animal Studies Committee in the Division of Comparative Medicine at Washington University School of Medicine. Laboratory procedures including viral vectors were approved by the Biosafety Committee at Washington University School of Medicine. Human fibroblasts were obtained from Coriell as a deidentified cell line under a Materials Transfer Agreement.

Data availability. All data shown in the figures are provided in a Supporting Data Values file (Microsoft Excel format).

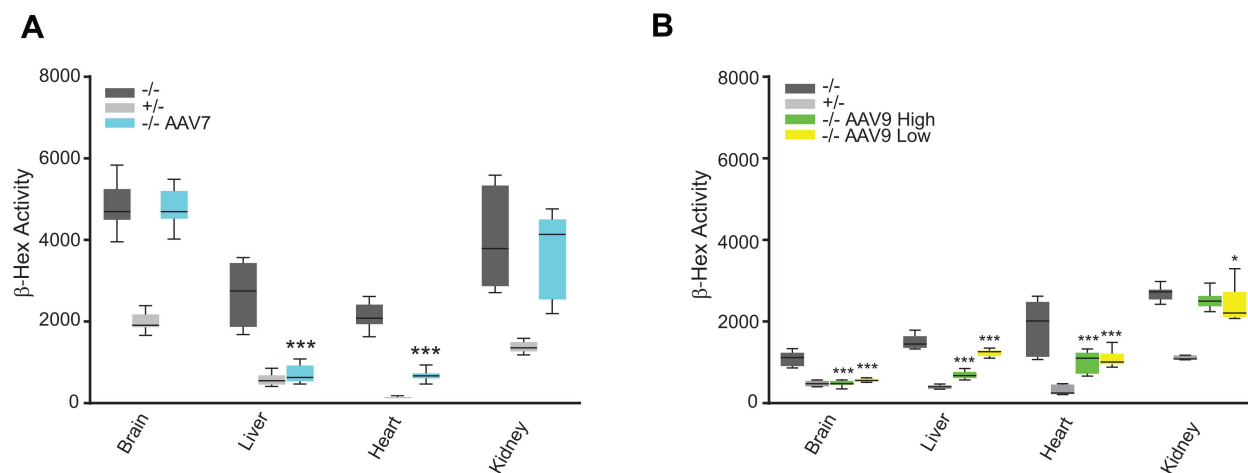
Acknowledgements. Support was provided by 1RM1 NS132962 to P.I.D. and J.D.C., 1R38 AI174266 to G.A., and by the Hope Center Viral Vectors Core at Washington University School of Medicine. This work is the result of NIH funding, in whole or in part, and is subject to the NIH Public Access Policy. Through acceptance of this federal funding, the NIH has been given a right to make the work publicly available in PubMed Central.

Author contributions. S.Q.L., B.D., J.D.C, and P.I.D. designed experiments, analyzed data, and wrote the manuscript. S.Q.L. and A.S. conducted murine experiments. S.S. and B.D. designed vectors. G.A. analyzed data. S.S. conducted in vitro experiments. S.Q.L. and G.J. performed immunofluorescence staining and biochemical assays. All authors reviewed and edited the manuscript.

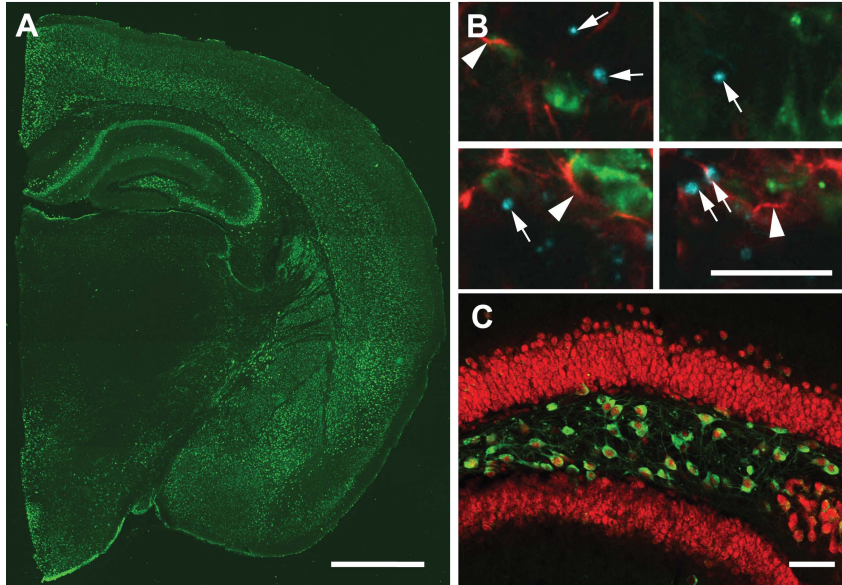
Supplemental Figures



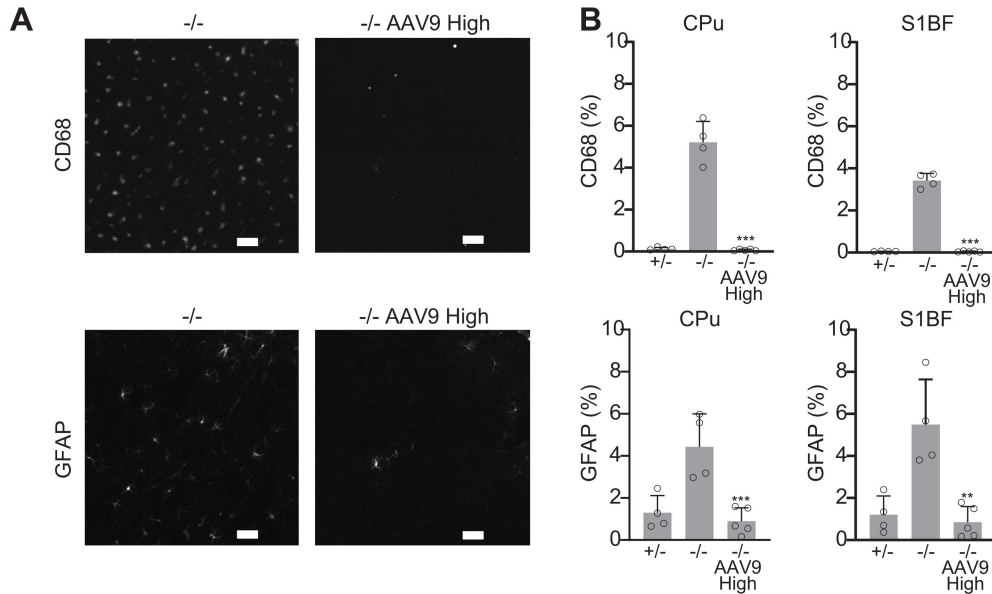
Supplemental Figure 1. *In vitro* expression of NAGLU-LAMP1 in human fibroblasts. (A) Schematic of construct. Human NAGLU cDNA, 6 glycine spacer (6G), transmembrane domain of lysosomal-associated membrane protein-1 (LAMP1), and c-myc, flanked by restriction sites Sall and XhoI. (B) GM 1426 cells (human MPS IIIB fibroblasts) were transduced in 24-well plates with lentiviral (LV) NAGLU-LAMP1. After washing the cells, media and cell pellets were each assayed. NAGLU activity represents mean and SD of 2 experiments and demonstrates that the construct is enzymatically active and not secreted. Beta-hexosaminidase activity in GM 1426 cells and media suggesting the construct is able to catabolize lysosomal substrate.



Supplemental Figure 2. Beta hexosaminidase activity in treated *Naglu*^{-/-} mice and controls. **(A)** Enzymatic activity of total beta-hexosaminidase (“β-Hex”) in organs of 8 wk old *Naglu*^{-/-} mice ($n=12$: 8 females, 4 males) treated at 4 wk of age with AAV7-NAGLU-LAMP1 (“AAV7”) intravenously, compared to untreated *-/-* ($n = 10$: 5 females, 5 males) and *+/-* ($n=10$: 5 females, 5 males) mice. **(B)** Total beta-hexosaminidase activity in organs of 4 wk old *Naglu*^{-/-} mice treated intracerebroventricularly at P1 or P2 with 6.5E9 vector genomes AAV9-Syn1-NAGLU-LAMP1 (“AAV9-Low;” $n = 8$: 4 females, 4 males) or 6.5E10 vector genomes AAV9-Syn1-NAGLU-LAMP1 (“AAV9-High;” $n = 13$: 3 females, 10 males), compared to untreated *-/-* ($n = 8$: 2 females, 6 males) and *+/-* ($n = 7$: 3 females, 4 males) mice. Means and S.D. shown. $**P < 0.01$ and $***P < 0.001$ vs *-/-* by pairwise comparisons of means.



Supplemental Figure 3: Immunofluorescence staining demonstrating cellular and tissue localization of NAGLU following intracerebral injection of $6.5E10$ vector genomes (high dose) AAV9-Syn1-NAGLU-LAMP1. **(A)** Anti-NAGLU staining (green) of a coronal hemispheric section of brain neocortex. Scalebar: $1000\ \mu\text{m}$. **(B)** Absence of colocalization of NAGLU staining (green) with staining for CD68 (cyan, arrows) or GFAP (red, arrowheads). Scalebar: $50\ \mu\text{m}$. **(C)** Cellular colocalization of NAGLU staining (green) with neuronal nuclei (red). Scalebar: $100\ \mu\text{m}$.



Supplemental Figure 4. Quantitative immunofluorescence staining for activated microglia (CD68) and astrocytosis (GFAP) in 4 wk old *Naglu*^{-/-} mice treated at P1 or P2 with 6.5E10 vector genomes AAV9-Syn1-NAGLU-LAMP1 (“AAV9-High,” *n* = 5: 2 females, 3 males) intracerebroventricularly, compared to untreated *-/-* (*n* = 4: 1 female, 3 males) and +/- (*n* = 4: 2 females, 2 males) mice. (A) Immunofluorescence staining for CD68 or GFAP at 10x magnification. Scalebar: 50 μ m. (B) Quantification of immunofluorescence staining. Bars represent means and S.D. of immunofluorescence intensity above threshold as a percentage of the area evaluated. ***P* < 0.01 and ****P* < 0.001 vs *-/-* by pairwise comparisons of means.

Supplemental References

1. Li HH, et al. Mouse model of Sanfilippo syndrome type B produced by targeted disruption of the gene encoding alpha-N-acetylglucosaminidase. *Proc Natl Acad Sci USA*. 1999;96 (25):14505-14510.
2. Yang H, et al. Rescue of GM3 synthase deficiency by spatially controlled, rAAV-mediated ST3GAL5 delivery. *JCI Insight*. 2023;8(9):e168688.
3. Weber-Adrian D, et al. Systemic AAV6-synapsin-GFP administration results in lower liver biodistribution, compared to AAV1&2 and AAV9, with neuronal expression following ultrasound-mediated brain delivery. *Sci Rep*. 2021;11(1):1934.
4. Kan SH, et al. Biochemical evaluation of intracerebroventricular rhNAGLU-IGF2 enzyme replacement therapy in neonatal mice with Sanfilippo B syndrome. *Mol Genet Metab*. 2021;133(2):185-192.
5. Marsh J, Fensom AH. 4-methylumbelliferyl α -N-acetylglucosaminidase activity for diagnosis of Sanfilippo B disease. *Clin Genet*. 2008;27(3):258-262.
6. Lawrence R, et al. Glycan-based biomarkers for mucopolysaccharidoses. *Mol Genet Metab*. 2014;111(2):73-83.
7. Nelvagal HR, et al. Cross-species efficacy of enzyme replacement therapy for CLN1 disease in mice and sheep. *J Clin Invest*. 2022;132(20):e163107.
8. Pearse Y, et al. Brain transplantation of genetically corrected Sanfilippo type B neural stem cells induces partial cross-correction of the disease. *Mol Ther Methods Clin Dev*. 2022;27:452-463.
9. Takahashi K, et al. Gene therapy ameliorates spontaneous seizures associated with cortical neuron loss in a Cln2R207X mouse model. *J Clin Invest*. 2023;133(12):e165908.